

Contractive Schrödinger cat states for a free mass

Lorenza Viola^{1,*} and Roberto Onofrio^{2,3,1,†}

¹*Los Alamos National Laboratory, Los Alamos, NM 87545, USA*

²*Dipartimento di Fisica “G. Galilei”, Università di Padova, via Marzolo 8, 35131 Padova, Italy*

³*Istituto Nazionale di Fisica della Materia, Unità di Roma “La Sapienza”,
and Center for Statistical Mechanics and Complexity, Piazzale A. Moro 2, Roma 00185, Italy*

(Dated: July 19, 2018)

Contractive states for a free quantum particle were introduced by Yuen (Yuen H P 1983 Phys. Rev. Lett. **51**, 719) in an attempt to evade the standard quantum limit for repeated position measurements. We show how appropriate families of two- and three component “Schrödinger cat states” are able to support non-trivial correlations between the position and momentum observables leading to contractive behavior. The existence of contractive Schrödinger cat states is suggestive of potential novel roles of non-classical states for precision measurement schemes.

PACS numbers: 03.65.-w, 03.65.Ta

I. INTRODUCTION

Shortly after the seminal paper by Schrödinger in 1935 [1], “Schrödinger cat” became a pictorial way to refer to a prototypical family of genuinely non-classical states *i.e.*, quantum states without a classical counterpart. While the introduction of such states found its original motivation in the analysis of the celebrated cat *Gedankenexperiment* in quantum measurement theory [1, 2], the quantum-mechanical weirdness of Schrödinger cat states has since then been widely appreciated in various contexts. The latter range from quantum non-locality [3], to non-classical states of light and matter [4], and to the emergence of classicality from the quantum world [5, 6]. In particular, cat states arising from the superposition of macroscopically distinguishable states of a quantum degree of freedom play a prominent role in the debate on macroscopic quantum mechanics [7]. More recently, the rapid development in the field of quantum information science [8] has prompted the consideration of various classes of non-classical states from the point of view of the quantum resources that they may involve [9, 10, 11]. For instance, cat-like superpositions of bosonic coherent states have been shown to provide robust encodings against amplitude damping [12], to carry the potential for improving the sensitivity of weak-force detection [13], as well as to exhibit generalized entanglement properties [14].

While applications of non-classical states within quantum information processing are still emerging, their association with the field of high precision measurements has a long history. A leading motivation stems from the need for understanding the ultimate resolution limitations for repeated position measurements in experimental and observational gravitation [15]. Without a careful preparation of the initial state, quantum mechanics sets a limit based on the assignment of equal uncertainties to position and momentum, resulting in the so-called *Standard Quantum Limit* (SQL) [16, 17]. Attempts to beat the SQL have stimulated the development of a theory for quantum non-demolition measurements [18, 19], and several experimental proposals aimed at improving the sensitivity of resonant detectors of gravitational radiation [20]. Efforts have primarily focused on a harmonic oscillator [19], resulting in the possibility of overcoming the SQL using non-classical

*Electronic address: lviola@lanl.gov

†Electronic address: onofrio@pd.infn.it

squeezed states. The case of a free test mass did not receive much attention until Yuen proposed a novel class of so-called *contractive states* analogous to the bosonic two-photon coherent states [21] and capable, in principle, of narrowing the position variance below the SQL bound. While Yuen's proposal initiated a controversial debate [22, 23, 24, 25, 26, 27, 28], the demand for schemes able to beat the SQL for free masses has meanwhile increased due to the amazing improvements in the sensitivity of gravitational wave interferometric detectors [29]. In principle, even a modest gain in the sensitivity obtainable by exploiting non-classical states would imply a relatively large increase in the fiducial volume for gravitational wave detection [30, 31, 32]. Unfortunately, contractive states as proposed by Yuen are difficult to produce in practice; the only concrete proposal that has appeared so far in the literature was regarding their generation for atomic states [33].

In this paper, we revisit Schrödinger cat states from the motivating perspective of the SQL of a free mass, and show how in addition to their already known properties they are also capable of manifesting contractive features. The content is organized as follows. In Section II we summarize the basic notions about the contractivity property as introduced by Yuen. In Section III we investigate the behavior of the position variance for a paradigmatic class of Schrödinger cat states, evidencing its dependence upon various parameters, and then outlining possible directions for generalization of this result. Section IV is devoted to discussing some implications of the existence of contractive Schrödinger cat states, and preliminarily assessing the prospects for demonstrating contractive cat behavior. Additional remarks are presented in the conclusions.

II. CONTRACTIVITY AND YUEN STATES

Consider a quantum particle of mass m freely evolving in one dimension. If \hat{x}, \hat{p} are the position and momentum observables, the equation of motion for \hat{x} in the Heisenberg picture is given by

$$\hat{x}(t) = \hat{x}(0) + \frac{\hat{p}(0)}{m} t, \quad t \geq 0. \quad (1)$$

Let Δx^2 and Δp^2 denote the variances of the corresponding operators *i.e.*, $\Delta x^2 = \langle \Delta \hat{x}^2 \rangle$, $\Delta p^2 = \langle \Delta \hat{p}^2 \rangle$, with $\Delta \hat{x} = \hat{x} - \langle \hat{x} \rangle$, $\Delta \hat{p} = \hat{p} - \langle \hat{p} \rangle$, and $\langle \hat{x} \rangle$, $\langle \hat{p} \rangle$ being the average position and momentum values, respectively. According to Eq. (1), the position variance after a time t can be related to the initial uncertainties $\Delta x^2(0)$ and $\Delta p^2(0)$ by

$$\Delta x^2(t) = \Delta x^2(0) + \frac{\Delta p^2(0)}{m^2} t^2 \geq \Delta x^2(0), \quad (2)$$

expressing the fact that the initial position variance increases under free evolution. The SQL for position measurements coincides with the minimum value attainable by $\Delta x^2(t)$ in (2) when t is regarded as the time interval between two successive, identical position measurements [23]. The argument is based on a heuristic application of the Heisenberg uncertainty principle, whereby $\Delta x(0)$ is interpreted as the uncertainty due to the finite resolution of the first measurement, and $\Delta p(0)$ represents the momentum disturbance caused by the measurement (see, however, [28] for a substantially more refined treatment). Because $\Delta x(0)\Delta p(0) \geq \hbar/2$, Eq. (2) can be rewritten as

$$\Delta x^2(t) \geq \Delta x^2(0) + \frac{\hbar^2 t^2}{4m^2 \Delta x^2(0)}, \quad (3)$$

which, upon minimization with respect to $\Delta x^2(0)$, implies

$$\Delta x^2(t) \geq \frac{\hbar t}{m} = \Delta x_{SQL}^2(t). \quad (4)$$

Accordingly, the outcome of the second position measurement cannot be predicted with uncertainty smaller than the SQL value, $\Delta x(t)_{SQL} = (\hbar t/m)^{1/2}$.

Yuen pointed out a major flaw in the above derivation, as by adding in quadrature the initial position variance and the one propagated in time from the initial momentum variance as in Eq. (2) it is implicitly assumed that position and momentum are initially uncorrelated. While this is correct, for instance, in the common case where the mass starts in a minimum-uncertainty state, it is necessary in general to relax this assumption, by replacing (2) with the full expression:

$$\begin{aligned} \Delta x^2(t) &= \langle \psi(0) | \hat{x}(t)^2 | \psi(0) \rangle - \langle \psi(0) | \hat{x}(t) | \psi(0) \rangle^2 \\ &= \Delta x^2(0) + \frac{\langle \{\Delta \hat{x}(0), \Delta \hat{p}(0)\} \rangle}{m} t + \frac{\Delta p^2(0)}{m^2} t^2, \end{aligned} \quad (5)$$

where $\{, \}$ denotes the anti-commutator operation. Thus, the position variance is directly sensitive to the initial *correlation coefficient* $\Delta_{xp}^2(0)$, with

$$\Delta_{xp}^2(0) = \langle \{\Delta \hat{x}(0), \Delta \hat{p}(0)\} \rangle = \langle \{\hat{x}, \hat{p}\} \rangle - 2\langle \hat{x} \rangle \langle \hat{p} \rangle = -i\hbar + 2\langle \hat{x} \hat{p} \rangle - 2\langle \hat{x} \rangle \langle \hat{p} \rangle, \quad (6)$$

upon explicitly using the canonical commutation rules for \hat{x}, \hat{p} [34]. Yuen also proposed an explicit class of quantum states, the so-called *twisted coherent states*, where a *negative* correlation term $\Delta_{xp}^2(0) < 0$ is realized [21]. As a consequence of the parabolic dependence of $\Delta x^2(t)$ upon t implied by (5), the initial position variance then narrows, attaining a minimum at an optimal time $\bar{t} > 0$. In addition, the variance remains below its initial value $\Delta x^2(0)$ for the finite time interval $0 < t < 2\bar{t}$, opening the possibility to evade the SQL for appropriate values of the parameters.

It is interesting to note that the essence of Yuen's proposal relies on allowing *complex* Gaussian states. In one dimension, for instance, consider a wave function of the form

$$\psi(x) = k \exp(-\alpha x^2), \quad (7)$$

with $\alpha \in \mathbb{C}$. By writing $\alpha = \alpha_1 + i\alpha_2$, $\alpha_1, \alpha_2 \in \mathbb{R}$, the normalization condition leads to $k = (2\alpha_1/\pi)^{1/4}$ (up to an irrelevant phase factor). Because for such a state $\langle \hat{x} \rangle = 0$, $\langle \hat{p} \rangle = 0$, and $\langle \hat{x} \hat{p} \rangle = i\hbar\alpha/2\alpha_1$, the corresponding correlation coefficient becomes

$$\Delta_{xp}^2(0) = \hbar \frac{\alpha - \alpha_1}{\alpha_1} = -2\hbar\xi, \quad (8)$$

where the parameter $\xi = \alpha_2/2\alpha_1$ can be, in principle, arbitrarily large. Note that the value $\xi = 0$ corresponds to the standard Gaussian state, while $\xi > 0$ implies a negative correlation term responsible for the desired non-monotonic behavior of $\Delta x^2(t)$. Following Yuen's notation, the prototype wave function (7) can be generalized to the following family of states:

$$\psi_Y(x) = \left(\frac{m\omega}{\pi\hbar|\mu - \nu|^2} \right)^{1/4} \exp \left\{ -\frac{m\omega}{2\hbar} \frac{1 + i2\xi}{|\mu - \nu|^2} (x - x_0)^2 + i\frac{p_0}{\hbar} (x - x_0) \right\}, \quad (9)$$

where now $\langle \hat{x} \rangle_Y = x_0$, $\langle \hat{p} \rangle_Y = p_0$ are real numbers, and the parameters μ, ν , and ω are related to the initial position and momentum variances and correlation as follows:

$$\Delta x_Y^2(0) = \frac{\hbar}{2m\omega} |\mu - \nu|^2, \quad (10)$$

$$\Delta p_Y^2(0) = \frac{\hbar m\omega}{2} \frac{1 + 4\xi^2}{|\mu - \nu|^2}, \quad (11)$$

$$\Delta_{xp,Y}^2(0) = -2\hbar\xi. \quad (12)$$

Note that $\alpha_1 = m\omega/2\hbar|\mu - \nu|^2$ (compare Eq. (7)), and the position variance evolves explicitly in time as:

$$\Delta x_Y^2(t) = \frac{\hbar}{2m\omega}|\mu - \nu|^2 - \frac{2\hbar\xi}{m}t + \frac{\hbar\omega}{2m} \frac{1 + 4\xi^2}{|\mu - \nu|^2} t^2. \quad (13)$$

Motivated by the comparison with the SQL, a natural strategy is to optimize the *relative* variance obtained upon normalizing $\Delta x_Y^2(t)$ by the spreading expected at time t for a state evolving at the SQL as given in (4) *i.e.*, to minimize the quantity

$$\Lambda_Y(t) \equiv \frac{\Delta x_Y^2(t)}{\Delta x_{SQL}^2(t)} = m \frac{\Delta x_Y^2(t)}{\hbar t}. \quad (14)$$

By differentiating $\Lambda_Y(t)$, we get a minimum relative variance at a time

$$t_Y^* = \frac{|\mu - \nu|^2}{\omega(1 + 4\xi^2)^{1/2}}. \quad (15)$$

This criterion coincides, for large values of ξ , with the direct optimization of the absolute variance (13) originally adopted in [21]:

$$\bar{t}_Y = \frac{2\xi|\mu - \nu|^2}{\omega(1 + 4\xi^2)}, \quad (16)$$

thanks to the fact that the ratio $t_Y^*/\bar{t}_Y = (1 + 4\xi^2)^{1/2}/2\xi$ quickly approaches unity with increasing ξ . The relative criterion (14), however, has the advantage of allowing for a continuous comparison with the SQL value at a generic instant of time t . From equations (13) and (15), the minimum relative variance is therefore

$$\Lambda_Y(t^*) = (1 + 4\xi^2)^{1/2} - 2\xi, \quad (17)$$

which quantifies the advantage in the use of a Yuen contractive state with respect to one with zero (or positive) correlations. As a function of ξ , the ratio in (17) is monotonically decreasing in the contractivity region $\xi > 0$, a unit value corresponding to a classical state with $\xi = 0$. While arbitrarily small values can be attained asymptotically, a significant gain already appears for relatively small ξ parameters; for instance $\Lambda_Y(t_Y^*) \simeq 0.41$ for $\xi = 1/2$.

As mentioned, Yuen's proposal sparked a lively debate on the meaning and conceptual consistency of the SQL for a free mass [22, 23, 24, 25, 26], and the discussion still continues [27, 28]. While various issues have been substantially elucidated, from an operational perspective limited effort has been devoted to address possible ways for preparing Yuen states in the laboratory. To the best of our knowledge, the only steps in this direction have been taken by Storey and co-workers [33], who proposed a position measurement scheme for atoms entering a strongly detuned standing light wave in a cavity, and by Vitali *et al.* [35] in the context of stochastic cooling of macroscopic mirrors. Ultimately, one obstacle encountered in designing realizable preparation schemes for Yuen states is related to the difficulty of dealing with a complex α . Thus, although very interesting in principle, this class of states seems not very palatable to experimentalists, motivating the search for alternative families of contractive states.

III. CONTRACTIVE FEATURES OF SCHRÖDINGER CAT STATES

Following Yuen's original suggestion, position-contractive states for a free mass are defined by the property

$$\left. \frac{d}{dt} \Delta x^2(t) \right|_{t=0} = \Delta_{xp}^2(0) < 0. \quad (18)$$

Because of the equation of motion (5), $\Delta x^2(t)$ increases monotonically with time whenever $\Delta_{xp}^2(0) \geq 0$. Equivalently, in terms of the relative variance $\Lambda(t)$, one may verify that if $\Delta_{xp}^2(0) \geq 0$, the inequality $\Lambda(t) \geq 1$ for all t is also enforced as a consequence of the Heisenberg uncertainty principle, and vice versa. In particular, the condition (18) is never satisfied by a preparation in a classical Gaussian state. However, Yuen's class is not the only family of non-classical Gaussian states one may *a priori* consider. Another notable class capable, as we shall describe now, of fulfilling (18) is provided by *macroscopically distinguishable* Gaussian states *i.e.*, Schrödinger cat states in the position variable.

A. Two-component cat states

Let us consider, to begin with, a two-component Schrödinger cat state, namely a coherent superposition of two one-dimensional Gaussian wave packets with inverse variance parameter $\alpha \in \mathbb{R}^+$, localized around two positions $+x_0$ and $-x_0$, $x_0 > 0$, and having relative amplitudes $k_+, k_- \in \mathbb{C}$:

$$\psi_{S2}(x) = N_2 \{ k_+ \exp[-\alpha(x - x_0)^2] + k_- \exp[-\alpha(x + x_0)^2] \}. \quad (19)$$

Here, the normalization constant is given by

$$|N_2|^2 = (2\alpha/\pi)^{1/2} [|k_+|^2 + |k_-|^2 + \exp(-2\alpha x_0^2)(k_+^* k_- + k_-^* k_+)]^{-1}, \quad (20)$$

and we have assumed that the two Gaussians have zero initial momentum. Note that, with this notation, each macroscopically distinguishable component in $|\psi_{S2}(x)|^2$ corresponds to a Gaussian probability distribution with variance $1/4\alpha$. After straightforward calculations we obtain the initial average values of position, momentum, and their product as follows:

$$\langle \hat{x} \rangle_{S2} = \frac{|k_+|^2 - |k_-|^2}{|k_+|^2 + |k_-|^2 + \exp(-2\alpha x_0^2)(k_+^* k_- + k_-^* k_+)} x_0, \quad (21)$$

$$\langle \hat{p} \rangle_{S2} = 4\hbar\alpha \frac{\text{Im}(k_+ k_-^*)}{|k_+|^2 - |k_-|^2} \exp(-2\alpha x_0^2) \langle \hat{x} \rangle_{S2}, \quad (22)$$

$$\langle \hat{x} \hat{p} \rangle_{S2} = i\hbar/2. \quad (23)$$

Thus, the correlation coefficient for a mass initially prepared in the state (19) is:

$$\Delta_{xp,S2}^2(0) = -2\langle \hat{x} \rangle_{S2} \langle \hat{p} \rangle_{S2} = -8\hbar\alpha \frac{\text{Im}(k_+ k_-^*)}{|k_+|^2 - |k_-|^2} \exp(-2\alpha x_0^2) \langle \hat{x} \rangle_{S2}^2. \quad (24)$$

According to (24), two contractivity regions fulfilling (18) are then possible in principle:

$$(I) \quad \begin{cases} |k_+|^2 - |k_-|^2 > 0, \\ \text{Im}(k_+ k_-^*) > 0, \end{cases} \quad \text{or} \quad (II) \quad \begin{cases} |k_+|^2 - |k_-|^2 < 0, \\ \text{Im}(k_+ k_-^*) < 0. \end{cases} \quad (25)$$

This illustrates a different route for generating a non-zero correlation coefficient compared to Yuen states. In the latter case, regardless of whether $\langle \hat{x} \rangle_Y \langle \hat{p} \rangle_Y = 0$ or not, a non-zero correlation $\Delta_{xp,Y}^2$ arises due to the asymmetric contribution from $\langle \hat{x} \hat{p} \rangle_Y$ and $\langle \hat{p} \hat{x} \rangle_Y$, enforcing $\langle \{ \hat{x}, \hat{p} \} \rangle_Y \neq 0$. For Schrödinger cat states of the form (19), it is instead the initial anti-correlation between \hat{x} and \hat{p} , $\langle \{ \hat{x}, \hat{p} \} \rangle_{S2} = 0$, that induces contractivity for appropriate k_+, k_- and $\langle \hat{x} \rangle_{S2} \neq 0$. From a less formal viewpoint, in the case of the Yuen states the presence of an imaginary part in the quadratic coefficient α effectively correlates the position and momentum observables. For cat states as in (19), the correlation is obtained through the *delocalized spatial structure*, which can enforce non-zero average values for both \hat{x} and \hat{p} as in (21)-(22).

In order to evaluate the position variance at time t based on (5), it is necessary to further calculate the second moments $\Delta x_{S2}^2(0)$ and $\Delta p_{S2}^2(0)$ (see also the appendix). For convenience, we set $\alpha = 1/2\Delta_0^2$ henceforth, and introduce an adimensional time parameter as

$$\eta = \frac{\hbar t}{m\Delta_0^2}. \quad (26)$$

It is worth noting that while the values of x_0 and Δ_0 separately affect the expectations $\langle \hat{x} \rangle_{S2}$, $\langle \hat{p} \rangle_{S2}$, the correlation coefficient (and hence contractivity) depends only upon their ratio, which we denote by $\delta = x_0/\Delta_0$. We can also assume, without loss of generality, that $k_+ \in \mathbb{R}$. By letting $k_+ = c_+$, $k_- = c_- e^{-i\theta}$, with $c_{\pm}, \theta \in \mathbb{R}$ and θ determining the initial relative phase between the two Gaussian components, we finally reach the rewritten forms:

$$\Delta x_{S2}^2(0) = \frac{\Delta_0^2}{2} + 2c_+c_- \frac{2c_+c_- + (c_+^2 + c_-^2)e^{-\delta^2} \cos \theta}{D} x_0^2, \quad (27)$$

$$\Delta p_{S2}^2(0) = \frac{\hbar^2}{\Delta_0^4} \left[\frac{\Delta_0^2}{2} - 2c_+c_- \frac{2c_+c_- e^{-\delta^2} + (c_+^2 + c_-^2) \cos \theta}{D} e^{-\delta^2} x_0^2 \right]. \quad (28)$$

In the above equations, $D = [c_+^2 + c_-^2 + 2c_+c_- e^{-\delta^2} \cos \theta]^2$. The complete expression for the position variance is then:

$$\begin{aligned} \Delta x_{S2}^2(\eta) &= \left[\frac{\Delta_0^2}{2} + 2c_+c_- \frac{2c_+c_- + (c_+^2 + c_-^2)e^{-\delta^2} \cos \theta}{D} x_0^2 \right] - \left[4c_+c_- \frac{c_+^2 - c_-^2}{D} \sin \theta e^{-\delta^2} x_0^2 \right] \eta \\ &+ \left[\frac{\Delta_0^2}{2} - 2c_+c_- \frac{2c_+c_- e^{-\delta^2} + (c_+^2 + c_-^2) \cos \theta}{D} e^{-\delta^2} x_0^2 \right] \eta^2. \end{aligned} \quad (29)$$

Thus, the variance may be written as $\Delta x_{S2}^2(\eta) = A + B\eta + C\eta^2$, where the coefficients **A**, **B**, **C** of the relevant powers of η can be inferred from the quantities in square brackets in Eq. (29). By construction, **A** reproduces the initial position variance, while **B** and **C** are responsible for the spreading from the initial value. The behavior for a single initial Gaussian state may be recovered by simply setting either c_+ or c_- to zero. Note that, regardless of possible contractive features, the rate of spreading of $\Delta x_{S2}^2(\eta)$ may be slower than in the Gaussian case due to the interference term contained in **C**. By normalizing $\Delta x_{S2}^2(\eta)$ to the reference value dictated by the SQL, $\Delta x_{SQL}^2(\eta) = \Delta_0^2 \eta$, we obtain:

$$\Lambda_{S2}(\eta) = \frac{\Delta x_{S2}^2(\eta)}{\Delta x_{SQL}^2(\eta)} = \frac{A_2}{\eta} + B_2 + C_2 \eta, \quad (30)$$

where $\mathbf{A}_2 = \mathbf{A}/\Delta_0^2$ etc. By minimizing $\Lambda_{S2}(\eta)$ with respect to η , an optimal time equal to $\eta^* = (\mathbf{A}_2/\mathbf{C}_2)^{1/2}$ is found, which is independent of the linear coefficient \mathbf{B}_2 . The corresponding minimum value attained by Λ_{S2} is

$$\Lambda_{S2}(\eta^*) = \mathbf{B}_2 + 2(\mathbf{A}_2\mathbf{C}_2)^{1/2}, \quad (31)$$

which can be further optimized with respect to the remaining parameters.

To analyse in detail the behavior of Λ_{S2} , it is convenient to additionally introduce the ratio $\kappa = c_+/c_-$, and rewrite the relative variance (29) as:

$$\begin{aligned} \Lambda_{S2}(\eta, \kappa, \theta, \delta) = & \left[\frac{1}{2} + 2\kappa\delta^2 \frac{2\kappa + (1 + \kappa^2)e^{-\delta^2} \cos \theta}{(1 + \kappa^2 + 2\kappa e^{-\delta^2} \cos \theta)^2} \right] \frac{1}{\eta} + \left[4\kappa\delta^2 \frac{(1 - \kappa^2)e^{-\delta^2} \sin \theta}{(1 + \kappa^2 + 2\kappa e^{-\delta^2} \cos \theta)^2} \right] \\ & + \left[\frac{1}{2} - 2\kappa\delta^2 \frac{2\kappa e^{-\delta^2} + (1 + \kappa^2) \cos \theta}{(1 + \kappa^2 + 2\kappa e^{-\delta^2} \cos \theta)^2} e^{-\delta^2} \right] \eta, \end{aligned} \quad (32)$$

where the dependence of Λ_{S2} upon the relevant parameters has been made explicit, and the expressions in the square brackets now correspond to $\mathbf{A}_2, \mathbf{B}_2, \mathbf{C}_2$ of (30). According to (32), Λ_{S2} is a complicated function of both the time η and the various parameters κ, δ, θ which characterize the initial state. In terms of the new parametrization, the contractivity regions given in (25) become:

$$(I) \quad \left\{ \begin{array}{l} \kappa > 1, \\ \sin \theta > 0, \end{array} \right. \quad \text{or} \quad (II) \quad \left\{ \begin{array}{l} \kappa < 1, \\ \sin \theta < 0. \end{array} \right. \quad (33)$$

Note that the dependence upon θ is periodic, thus we can limit the analysis to the range $0^\circ \leq \theta < 360^\circ$. In addition, Λ_{S2} satisfies the following invariance property:

$$\Lambda_{S2}(\eta, \kappa, \theta, \delta) = \Lambda_{S2}(\eta, \kappa^{-1}, 360^\circ - \theta, \delta). \quad (34)$$

Thus, given the behavior of Λ_{S2} in a single contractivity region, say (I), the behavior in the remaining region is the same upon transforming $\kappa \mapsto \kappa^{-1}$ and $\theta \mapsto 360^\circ - \theta$. Some qualitative insights into the behavior of the function (32) can be obtained by inspection of the various terms. The contractive term, \mathbf{B}_2 , assumes zero values at $\theta = 0^\circ$ and 180° , namely, when the two distinguishable components of the cat add in phase or anti-phase, as well as when $\kappa = 1$, which corresponds to an equally weighted superposition state. As a function of θ and δ , $|\mathbf{B}_2|$ is large for $\theta \approx 90^\circ$ and δ of the order of unity.

By numerical analysis of Eq. (32), the figure of merit for contractivity Λ_{S2} is found to attain its minimum

$$\Lambda_{S2}^{min}(\eta^*, \kappa^*, \theta^*, \delta^*) \simeq 0.757, \quad (35)$$

for optimal parameter values $\eta^* \simeq 1.105$, $\kappa^* \simeq 2.26$, $\theta^* \simeq 127^\circ$, and $\delta^* \simeq 0.49$. The dependence of Λ_{S2} upon the effective time η and κ is displayed in Fig. (1) for $\theta = \theta^*$ and $\delta = \delta^*$. The section in the (η, κ) plane resulting from a cut with the plane $\Lambda_{S2} = 1$ is also depicted. The plot evidences a region where Λ_{S2} stays below 1. For comparison, in Figs. (2) and (3), the corresponding dependence is shown for a state which only differs in the initial relative phase, $\theta = 0^\circ$ and 180° , respectively. The region $\Lambda_{S2} < 1$ is not entered for such states.

By keeping the effective time fixed at the value $\eta = \eta^*$, one can focus on some other dependencies as illustrated in Figs. (4) and (5). In particular, Fig. (4) shows the dependence upon θ and κ . In this case, a reference contour plot is chosen at constant $\Lambda_{S2} = 0.8$. The two contractivity islands characterized by (33) are clearly visible, and related to each other as in (34). In Fig. (5), a similar plot depicts the dependences upon δ and κ .

B. Generalizations: Three-component cat states

The above analysis shows that contractive quantum states, in the original Yuen's spirit, can be engineered through an appropriate choice of parameters in the class of cat states described by (19). Several variants might be worth exploring in principle. For instance, cat states arising from the superposition of two Gaussians differing in their values of the parameters x_0 or Δ_0 , or possessing non-zero initial momenta could be examined, as well as superpositions of non-Gaussian wave-packets.

Another direction for generalizations is to consider *multi-component cat states*, for which contractivity could be enhanced via coherent interference effects between different pairs. We illustrate this possibility by focusing on the simplest generalization of the class (19), leading to a family of cat states with three macroscopically distinguishable components. Thus, let us consider a wave-function of the form

$$\psi_{S3}(x) = N_3 \left\{ k_+ \exp[-(x - x_0)^2/2\Delta_0^2] + k_0 \exp[-x^2/2\Delta_0^2] + k_- \exp[-(x + x_0)^2/2\Delta_0^2] \right\}, \quad (36)$$

where the normalization constant is now given by

$$|N_3|^2 = (\pi\Delta_0^2)^{-1/2} \left[|k_+|^2 + |k_0|^2 + |k_-|^2 + (k_+^* k_- + k_+ k_-^*) e^{-\delta^2} + (k_+^* k_0 + k_+ k_0^*) e^{-\delta^2/4} + (k_-^* k_0 + k_- k_0^*) e^{-\delta^2/4} \right]^{-1}. \quad (37)$$

Here, $\delta = x_0/\Delta_0$ as before, and we also continue to assume that the three Gaussians have zero initial momentum. Because a global phase factor is irrelevant, the state (36) is parametrized by five real parameters describing the relative amplitudes and phases, in addition to x_0 and Δ_0 , which are taken as before to be positive. Similar to the two-component cat case, we arbitrarily choose one of the k coefficients to be real, thus setting $k_0 = c_0$, $k_+ = c_+ e^{i\theta_+}$, $k_- = c_- e^{i\theta_-}$, with $c_0, c_{\pm}, \theta_{\pm} \in \mathbb{R}$. With these conventions, the results for two-component cat states of the previous section can be recovered by letting $c_0 = 0, \theta_+ = 0$, and $\theta_- = -\theta$. We also define

$$K = c_+^2 + c_0^2 + c_-^2 + 2c_0(c_+ \cos \theta_+ + c_- \cos \theta_-) e^{-\delta^2/4} + 2c_+ c_- \cos(\theta_+ - \theta_-) e^{-\delta^2}. \quad (38)$$

The expectations of the position and momentum observables on the state (36) take a more complicated form than in (21)-(22):

$$\langle \hat{x} \rangle_{S3} = \frac{1}{K} \left[c_+^2 - c_-^2 + c_0(c_+ \cos \theta_+ - c_- \cos \theta_-) e^{-\delta^2/4} \right] x_0, \quad (39)$$

$$\langle \hat{p} \rangle_{S3} = \frac{\hbar}{\Delta_0^2} \frac{c_0(c_+ \sin \theta_+ - c_- \sin \theta_-) e^{-\delta^2/4} + 2c_+ c_- \sin(\theta_+ - \theta_-) e^{-\delta^2}}{c_+^2 - c_-^2 + c_0(c_+ \cos \theta_+ - c_- \cos \theta_-) e^{-\delta^2/4}} \langle \hat{x} \rangle_{S3}. \quad (40)$$

Similarly, one also finds

$$\begin{aligned} \langle \hat{x}\hat{p} \rangle_{S3} &= i \frac{\hbar}{2K} \left[c_+^2 + c_0^2 + c_-^2 + 2c_0(c_+ \cos \theta_+ + c_- \cos \theta_-) e^{-\delta^2} \right. \\ &\quad \left. + 2c_+ c_- \cos(\theta_+ - \theta_-) e^{-\delta^2} - 2ic_0 \delta^2 (c_+ \sin \theta_+ + c_- \sin \theta_-) e^{-\delta^2/4} \right]. \end{aligned} \quad (41)$$

Thus, unlike in the ordinary cat case leading to Eq. (23), $\langle \hat{x}\hat{p} \rangle_{S3}$ acquires in general a non-vanishing real component. While one can verify that $\text{Im}(\langle \hat{x}\hat{p} \rangle_{S3}) = i\hbar/2$ and hence that a real value of the

correlation coefficient is correctly enforced, the full expression for $\Delta_{xp,S_3}^2(0)$ is less transparent than in the two-component case. In formal analogy to Eq. (12), we may write

$$\Delta_{xp,S_3}^2(0) = 2 \left(\text{Re}(\langle \hat{x}\hat{p} \rangle_{S_3}) - \langle \hat{x} \rangle_{S_3} \langle \hat{p} \rangle_{S_3} \right) = -2\hbar\zeta, \quad (42)$$

where

$$\zeta = \frac{\delta^2}{K^2} \left[-c_0(c_+ \sin \theta_+ + c_- \sin \theta_-) K e^{-\delta^2/4} + \left(c_0(c_+ \sin \theta_+ - c_- \sin \theta_-) e^{-\delta^2/4} + 2c_+c_- \sin(\theta_+ - \theta_-) e^{-\delta^2} \right) \left(c_+^2 - c_-^2 + c_0(c_+ \cos \theta_+ - c_- \cos \theta_-) e^{-\delta^2/4} \right) \right]. \quad (43)$$

The above function satisfies the property that

$$\zeta(c_+, c_-, \theta_+, \theta_-) = \zeta(c_-, c_+, \theta_-, \theta_+), \quad (44)$$

i.e., it is invariant under the exchange $k_+ \mapsto k_-$. Thus, one may expect ζ to be extremal for $k_+ = k_-$, or $c_+ = c_-$ and $\theta_+ = \theta_-$. The fact that under these conditions contractive behavior is possible for a cat state of the form (36) is easily verified by noting that $\langle \hat{x} \rangle_{S_3} = 0$, $\langle \hat{p} \rangle_{S_3} = 0$, and

$$\zeta_{[c_+=c_-; \theta_+=\theta_-]} = -2 \frac{\delta^2}{K} c_0 c_+ \sin \theta_+ e^{-\delta^2/4}. \quad (45)$$

Thus, $\zeta > 0$ for $\theta_+ \in (180^\circ, 360^\circ)$, which in turn corresponds to a family of cat states with a negative correlation term. Note that this is in contrast with the two-component case, where a non-vanishing expectation of \hat{x} (hence \hat{p}) was found to be necessary for contractivity.

The complete calculation of the position variance $\Delta_{S_3}^2(\eta)$ as a function of the rescaled time is slightly simpler in the Schrödinger representation in this case. The essential steps and final equations are quoted in the appendix. Working as before in terms of a relative variance,

$$\Lambda_{S_3}(\eta) = \frac{\Delta_{S_3}^2(\eta)}{\Delta_{S_{QL}}^2(\eta)} = \frac{\mathbf{A}_3}{\eta} + \mathbf{B}_3 + \mathbf{C}_3\eta, \quad (46)$$

explicit expressions for the coefficients $\mathbf{A}_3, \mathbf{B}_3, \mathbf{C}_3$ may be derived from the appendix. The behavior of Λ_{S_3} has been analyzed numerically in the parameter space corresponding to the set $\eta, \kappa_+, \kappa_-, \theta_+, \theta_-, \delta$, with $\kappa_+ = c_+/c_-$ and $\kappa_- = c_0/c_-$. In this case, the global optimization leads to a minimum value

$$\Lambda_{S_3}^{min}(\eta^*, \kappa_+^*, \kappa_-^*, \theta_+^*, \theta_-^*, \delta^*) \simeq 0.569, \quad (47)$$

for optimal parameter values $\eta^* \simeq 1.270$, $\kappa_+^* \simeq 1.00$, $\kappa_-^* \simeq 2.38$, $\theta_+^* \simeq 249^\circ$, $\theta_-^* \simeq \theta_+^*$, and $\delta^* \simeq 1.21$. The fact that $\kappa_+^* \simeq 1.00$ and $\theta_-^* \simeq \theta_+^*$ within the numerical accuracy indicates that the minimum of Λ_{S_3} is indeed attained in the parameter regime expected from (45). A pictorial comparison between the behavior of the optimized contractivity figures of merit $\Lambda_{S_2}^*$ and $\Lambda_{S_3}^*$ as a function of η for two- and three-component cat states is displayed in figure (6). Is it worth noting that not only $\Lambda_{S_3}^* < \Lambda_{S_2}^*$ for $\eta \gtrsim 0.5$, but also the region where values lower than one are achieved appreciably widens for three-component contractive cat states.

For an additional comparison between contractive and non-contractive behavior, it is also instructive to directly examine the time dependence of the absolute variance for representative two-, three-component cat states, and for a Gaussian wave-packet with the same width parameter Δ_0 . The results are shown in figure(7) for maximally contractive cat states. The monotonic increase of the variance for the Gaussian case,

$$\Delta x_G^2(\eta) = \frac{\Delta_0^2}{2} (1 + \eta^2), \quad (48)$$

is clearly visible. The SQL behavior of Eq. (4), which translates into $\Delta_{SQL}^2(\eta) = \Delta_0^2\eta$, is reached at time $\eta = 1$ in the non-contractive Gaussian case of (48). The contractivity intervals for two- and three-component cat states are determined by the appropriate intersections of the variance curves $\Lambda_{S_2}, \Lambda_{S_3}$ with the SQL-line. Viewed in this way, the advantage of contractive states also manifests itself in the ability to preserve variances comparable to the initial Gaussian value at later times. In addition, the stronger contractivity of a three-component cat state is evidenced by the higher initial slope, implying both a deeper excursion below the SQL value and a longer contractivity interval.

To summarize, the larger set of parameters available in more complex classes of Schrödinger cat states is capable of supporting stronger and better contractive properties. While further investigation is needed to precisely characterize all the possible configurations, the fact that states with increased complexity may allow for a richer “self-interference” pattern (and hereby enhanced contractivity) is likely to occur beyond the specific case examined here. In particular, this is also somewhat reminiscent of the recent findings in [36], where cat states such as “compass-like” superpositions of four Gaussians are able to probe sub-Planck structures in the phase space.

IV. IMPLICATIONS OF CONTRACTIVE CAT STATES

The existence of contractive cat states immediately evokes, as in Yuen’s original proposal, the potential for breaching the SQL of a free mass. However, a full assessment of such a potential requires a proper formulation of both the SQL itself and of various measurement-theoretical concepts such as quantum precision, resolution, and uncertainty. While addressing these issues goes beyond the scope of the present work, as far as the implications for the SQL are concerned we limit ourselves to a few preparatory remarks.

As emphasized by Ozawa [24], because the SQL applies to *repeated* quantum measurements, one essential ingredient is the ability to perform a measurement using a *single* measuring apparatus, the reading of which provides accurate information about the position of the free mass and simultaneously prepares it for the next position measurement, leaving it in a contractive state. A class of measurement schemes well suited for this task is offered by so-called *Gordon-Louisell (GL) position measurements* [37]. The latter are naturally described within the general formalism of quantum operations [8, 38]. Let $a \in \mathbb{R}$ be a real parameter, to be interpreted as the possible outcome of a position readout for a one-dimensional system, and let $\{|a\rangle\}$ denote the complete set of position eigenstates. If $\{\Psi_a\}$ is a family of normalized wave functions indexed by a , and $\rho(0^-)$ is the state of the system prior to the measurement, the state change and measurement statistics corresponding to a GL position measurement $\{|\Psi_a\rangle\langle a|\}$ are described by the following operation measure and effect measure, respectively:

$$\rho(0^+) = \int_I da A_a \rho(0^-) A_a^\dagger, \quad A_a = |\Psi_a\rangle\langle a|, A_a^\dagger = |a\rangle\langle \Psi_a|, \quad (49)$$

$$\text{Prob}(a \in I | \rho(0^-)) = \text{Trace} \left[\int_I da A_a^\dagger A_a \rho(0^-) \right] = \text{Trace} \left[\int_I da |a\rangle\langle a| \rho(0^-) \right], \quad (50)$$

for all Borel sets $I \subseteq \mathbb{R}$. The distinctive feature of GL position measurement is that, according to (49), the posterior state $\rho(0^+)$ of the system is determined by Ψ_a *regardless of the prior state* $\rho(0^-)$, the latter determining the outcome probabilities according to (50). Because GL measurements are described by completely-positive quantum maps, every GL measurement is physically realizable in principle [24].

GL contractive position measurements were originally invoked by Yuen [21]. Given contractive states of the form (9), the relevant family $\{\Psi_a\}_Y$ may be constructed by fixing the parameters μ, ν, ω , and by identifying $x_0 = \langle \hat{x} \rangle_Y = a$, for all real a . If we now look, for instance, at two-component cat states as in (19), then a contractive state satisfying that $\langle \hat{x} \rangle_{S_2} = a$ can be found except for the (zero-measure) set $I = \{a = 0\}$. Let $\beta > 1$ a positive number. Then one may define a family $\{\Psi_a\}_{S_2}$ as follows:

$$\{\Psi_a\}_{S_2} = \begin{cases} \{|\kappa_{>} = \sqrt{(\beta-1)/(\beta+1)}; \theta = 270^\circ; x_0 = \beta a, \Delta_0 = \beta a/\delta\} & a > 0, \\ \{|\kappa_{<} = \sqrt{(\beta+1)/(\beta-1)}; \theta = 90^\circ; x_0 = -\beta a, \Delta_0 = -\beta a/\delta\} & a < 0. \end{cases} \quad (51)$$

For fixed $|a|$, the two corresponding states in (51) have the same degree of contractivity thanks to the relationship (34). By choosing $\delta = \delta^*$ and adjusting β in such a way that $\kappa_{<} = \kappa^*$, $\kappa_{>} = 1/\kappa^*$, contractivity can then be brought close to optimality. Establishing whether a family of contractive cat states such as (51) actually supports a well-defined GL position measurement, and whether the latter may succeed in breaking the SQL, are interesting problems *per se*, which would call for an analysis along the lines of [24]. Once a successful strategy is identified in principle, an additional issue would be looking for an explicit interaction Hamiltonians implementing the desired contractive measurement scheme. For Yuen states, such a constructive problem was solved by Ozawa [24]. It is interesting to note that the proposed measurement model explicitly requires the initialization of the meter in a contractive state, and contractivity is subsequently transferred to the mass via a controlled interaction. In this context, cat states might then turn advantageous if preparation procedures simpler than the ones generating Yuen states could be exploited to appropriately initialize the meter.

Independently of the SQL motivation, the possibility of experimentally demonstrating and characterizing contractive behavior for a free massive particle is both interesting as a fundamental quantum property, and for its possible implications in high-precision *single* quantum measurements. While being certainly challenging with present capabilities, accomplishing this goal could largely benefit from the extensive efforts which are under way to realize Schrödinger cat states in diverse physical systems. Starting from the pioneering proposals by Yurke and Stoler [39, 40] for the generation of optical cat states, and related following proposals [41, 42], such efforts have led to the successful creation and manipulation of macroscopically distinguishable photon states in the cavity QED setting [4], and have culminated in the generation of a mesoscopic Schrödinger cat for a trapped Be ion [43]. Also, the creation of macroscopically distinguishable states has been recently reported for superconducting circuits [44, 45, 46], and proposals for entanglement of trapped electrons have been recently formulated [47]. Interesting proposals exist for generating Schrödinger cat states of mechanical systems via controlled entanglement with microscopic degrees of freedom, including electron pairs in Cooper boxes [48], single photons in beam-splitter configurations [49], as well as radiation-pressure controlled mirrors [50, 51, 52, 53, 54, 55]. Finally, recent advances in ultracold atom physics open new perspectives for the possibility of creating Schrödinger cat states with ultracold atomic ensembles or gaseous Bose-Einstein condensates [56, 57].

Devices based on trapped ions or cold atoms seem especially promising for demonstrating and exploiting contractivity properties. In this case, if one of the strategies mentioned above actually succeeds for engineering a contractive Schrödinger cat state, trapping potentials could be switched off and the mass (ion or atomic cloud) be released to free evolution for a given time interval. The position variance could then be inferred from the spatial pattern of the fluorescent light emitted under the action of a light probe beam, and by repeating the experiment for different times of flight the relevant time dependence could be reconstructed. Besides demonstration, contractivity might find useful applications in high-precision atomic physics experiments. For instance, one possibility worth exploring in principle is trying to improve the accuracy of atomic-fountain clocks through proper refocusing of the atomic cloud on the fluorescence detection area, as this could translate

into a decrease of the absolute uncertainty on the atomic populations [58]. A general observation which may be relevant in this context is that, because the behavior of the position variance would be unchanged for a mass subject to a linear potential, contractive states for a free mass would still exhibit contractivity under a *uniform gravitational field* (see also [59] for a related discussion). Thus, contractivity could in principle be exploited both in the vertical and horizontal directions.

In spite of these promising avenues, a potentially serious concern arises from the fact that Schrödinger cat states may be especially fragile against the decoherence effects caused by the coupling to their surrounding environment, a feature which is regarded as crucial to understanding the quantum-to-classical transition [5, 6]. Under the assumption that the environment may be schematized as a harmonic bosonic bath, exact analyses are possible by adapting the results available for the quantum Brownian motion model [6, 60], or by directly resorting to results already obtained for a free damped quantum particle [61, 62]. However, it is also worth stressing that the decoherence behavior may be quite sensitive to various details of the system-environment coupling as well as environment properties, and there is hope that on one hand estimates based on general models might be in some cases overly pessimistic [63], and on the other hand decoherence effects might be effectively counteracted. In particular, stabilization procedure for cat states could be in principle designed based on the basis of both active-control schemes for the system [64, 65] and symmetrization schemes for the environment [66].

V. CONCLUSIONS

We have shown that Schrödinger cat states provide a new class of states able to support contractive features in the sense originally proposed by Yuen in [21]. Yuen contractive states lead in principle to an unlimited gain with respect to the SQL for a free particle but, apart from a proposal in the atomic physics context [33], it is not clear how to prepare such states in practice. Contractive Schrödinger cat states, on the other hand, may enable one to capitalize on the intense effort which is ongoing to generate Schrödinger cat states with various quantum devices, ranging from trapped ions and atoms to superconducting circuits.

Viewed from a broader perspective, our results enforce the conclusions reached in [9], where the use of non-classical states and quantum resources of relevance for quantum information processing is also anticipated to improve our capabilities to gather information in high precision measurements. For Schrödinger cat states in particular, the identification of contractivity features provides independent additional support to the idea that highly delocalized states may develop enhanced quantum sensitivity as recently suggested by Zurek [36]. While several questions remain to be addressed in more depth, the present analysis thus points to a novel significance and potentially useful applications of Schrödinger cat states in the context of quantum-limited measurements.

Acknowledgments

L.V. gratefully acknowledges current support from the Los Alamos Office of the Director through a J. R. Oppenheimer Fellowship, and also wishes to thank the University of Padova for hospitality at the time in which these ideas originated. This work was also supported in part by Cofinanziamento MIUR protocollo MM02263577_001.

APPENDIX A: SCHRÖDINGER REPRESENTATION

For completeness, we report the evaluation of the position variance in the Schrödinger representation. For two-component Schrödinger cat states, the starting point is the wave function

$$\psi_{S2}(x, 0) = N_2 \{k_+ \exp[-(x - x_0)^2/2\Delta_0^2] + k_- \exp[-(x + x_0)^2/2\Delta_0^2]\},$$

where the normalization constant (also given in Eq. (20)) is

$$|N_2|^2 = (\pi\Delta_0^2)^{-1/2} \left[|k_+|^2 + |k_-|^2 + (k_+k_-^* + k_-^*k_+)e^{-\delta^2} \right]^{-1},$$

and, as before, $\delta = x_0/\Delta_0$. The time evolution is obtained by solving the Schrödinger equation with effective time η ,

$$\frac{\partial\psi}{\partial\eta} = i\frac{\Delta_0^2}{2} \frac{\partial^2\psi}{\partial x^2},$$

which is easily accomplished by Fourier expanding the Gaussian states in terms of plane waves (see also [59]). The resulting wave function may be written as:

$$\psi_{S2}(x, \eta) = N_2 \frac{\exp(-\frac{i}{2}\text{atan } \eta)}{(1 + \eta^2)^{1/4}} \left[k_+ \exp\left(-\frac{(1 - i\eta)(x - x_0)^2}{2\Delta_0(1 + \eta^2)}\right) + k_- \exp\left(-\frac{(1 - i\eta)(x + x_0)^2}{2\Delta_0(1 + \eta^2)}\right) \right].$$

Thus, the required first and second momenta of the position observable are calculated as:

$$\langle \hat{x} \rangle_{\psi_{S2}(x, \eta)} = |N_2|^2 (\pi\Delta_0^2)^{1/2} x_0 \left[|k_+|^2 - |k_-|^2 - i\eta(k_+k_-^* - k_-^*k_+)e^{-\delta^2} \right],$$

and

$$\begin{aligned} \langle \hat{x}^2 \rangle_{\psi_{S2}(x, \eta)} &= |N_2|^2 (\pi\Delta_0^2)^{1/2} \left[(|k_+|^2 + |k_-|^2) \left(\frac{(1 + \eta^2)\Delta_0^2}{2} + x_0^2 \right) + \right. \\ &\quad \left. + (k_+k_-^* + k_-^*k_+) \left(\frac{(1 + \eta^2)\Delta_0^2}{2} - \eta^2 x_0^2 \right) e^{-\delta^2} \right]. \end{aligned}$$

The position variance $\Delta x_{S2}^2(\eta) = \langle \hat{x}^2 \rangle_{\psi_{S2}(x, \eta)} - \langle \hat{x} \rangle_{\psi_{S2}(x, \eta)}^2$ agrees with the result (29) obtained from the Heisenberg representation.

In the case of three-component Schrödinger cat states as considered in Sect. IIIB, the initial wave function is

$$\psi_{S3}(x, 0) = N_3 \{k_+ \exp[-(x - x_0)^2/2\Delta_0^2] + k_0 \exp[-x^2/2\Delta_0^2] + k_- \exp[-(x + x_0)^2/2\Delta_0^2]\},$$

with N_3 (also quoted in Eq. (37)) given by

$$\begin{aligned} |N_3|^2 &= (\pi\Delta_0^2)^{-1/2} \left[|k_+|^2 + |k_0|^2 + |k_-|^2 + (k_+^*k_- + k_+k_-^*)e^{-\delta^2} \right. \\ &\quad \left. + (k_+^*k_0 + k_+k_0^*)e^{-\delta^2/4} + (k_-^*k_0 + k_-k_0^*)e^{-\delta^2/4} \right]^{-1}. \end{aligned}$$

The time-evolved wave function $\psi_{S3}(x, \eta)$ can again be evaluated by solving the above Schrödinger equation. After cumbersome but straightforward calculations we obtain the average values of the position and its square as follows:

$$\begin{aligned} \langle \hat{x} \rangle_{\psi_{S3}(x, \eta)} &= |N_3|^2 (\pi \Delta_0^2)^{1/2} x_0 \left[c_+^2 - c_-^2 + \frac{1}{2} (k_+^* k_0 + k_+ k_0^*) e^{-\delta^2/4} - \frac{1}{2} (k_-^* k_0 + k_- k_0^*) e^{-\delta^2/4} \right. \\ &\quad \left. + \left(\frac{i}{2} (k_+^* k_0 - k_+ k_0^*) e^{-\delta^2/4} + i (k_+^* k_- - k_+ k_-^*) e^{-\delta^2} - \frac{i}{2} (k_-^* k_0 - k_- k_0^*) e^{-\delta^2/4} \right) \eta \right] \end{aligned}$$

and

$$\begin{aligned} \langle \hat{x}^2 \rangle_{\psi_{S3}(x, \eta)} &= |N_3|^2 (\pi \Delta_0^2)^{1/2} \left[\frac{1}{2} (c_+^2 + c_0^2 + c_-^2) \Delta_0^2 (1 + \eta^2) + (c_+^2 + c_-^2) x_0^2 \right. \\ &\quad + \frac{1}{2} (k_+^* k_0 + k_+ k_0^*) e^{-\delta^2/4} \Delta_0^2 (1 + \eta^2) + \frac{1}{4} (k_+^* k_0 + k_+ k_0^*) e^{-\delta^2/4} x_0^2 (1 - \eta^2) \\ &\quad + \frac{i}{2} (k_+^* k_0 - k_+ k_0^*) e^{-\delta^2/4} x_0^2 \eta + \frac{1}{2} (k_+^* k_- + k_+ k_-^*) e^{-\delta^2} \Delta_0^2 (1 + \eta^2) + \\ &\quad - (k_+^* k_- + k_+ k_-^*) e^{-\delta^2} x_0^2 \eta^2 + \frac{1}{2} (k_-^* k_0 + k_- k_0^*) e^{-\delta^2/4} \Delta_0^2 (1 + \eta^2) \\ &\quad \left. + \frac{1}{4} (k_-^* k_0 + k_- k_0^*) e^{-\delta^2/4} x_0^2 (1 - \eta^2) + \frac{i}{2} (k_-^* k_0 - k_- k_0^*) e^{-\delta^2/4} x_0^2 \eta \right]. \end{aligned}$$

The position variance may be calculated from $\Delta x_{S3}^2(\eta) = \langle \hat{x}^2 \rangle_{\psi_{S3}(x, \eta)} - \langle \hat{x} \rangle_{\psi_{S3}(x, \eta)}^2$. By collecting terms of the same order in η and taking the ratio to the SQL value, the relative variance $\Lambda_{S3}(\eta)$ may be cast in the form (46). The above procedure was implemented numerically to calculate the optimal value Λ_{S3}^* and infer the corresponding parameters.

-
- [1] Schrödinger E 1935 Die gegenwärtige Situation in der Quantenmechanik *Naturwissenschaften* **23** 807. English translation available in 1980 *Proc. Am. Phil. Soc.* **124** 323
 - [2] Wheeler J A and Zurek W H 1983 *Quantum Theory and Measurement* (Princeton: Princeton University Press)
 - [3] Bell S J 1993 *Speakable and Unsayable in Quantum Mechanics* (Cambridge: Cambridge University Press)
 - [4] Raimond J M, Brune M and Haroche S 2001 Manipulating quantum entanglement with atoms and photons in a cavity *Rev. Mod. Phys.* **73** 565, and references therein
 - [5] Zurek W H 1982 Environment-induced superselection rules *Phys. Rev. D* **26** 1862; 1991 Decoherence and the transition from quantum to classical *Phys. Today* **44** 36; 1993 Negotiating the tricky border between quantum and classical: reply *Phys. Today* **46** 84
 - [6] Giulini D, Joos E, Kiefer C, Kupsch J, Stamatescu I-O, and H. D. Zeh 1996 *Decoherence and the Appearance of a Classical World in Quantum Theory* (Berlin: Springer-Verlag)
 - [7] Leggett A J 1980 Macroscopic quantum-systems and the quantum-theory of measurement *Suppl. Progr. Theor. Phys.* **69** 80; Leggett A J and Garg A 1985 Quantum-mechanics versus macroscopic realism: is the flux there when somebody looks? *Phys. Rev. Lett.* **54** 857
 - [8] Nielsen M A and Chuang I L 2000 *Quantum Computation and Quantum Information* (Cambridge: Cambridge University Press)
 - [9] Preskill J 2000 Quantum information and physics: some future directions *J. Mod. Opt.* **47** 127; Childs A M, Preskill J and Renes J 2000 Quantum information and precision measurement *ibid.* **47** 155
 - [10] Huelga S F, Macchiavello C, Pellizzari T and Ekert A K 1997 Improvement of frequency standards with quantum entanglement *Phys. Rev. Lett.* **79** 3865
 - [11] Meyer V, Rowe M A, Kielpinski D, Sackett C A, Itano W M, Monroe C and Wineland D J 2001 Experimental demonstration of entanglement-enhanced rotation angle estimation using trapped ions *Phys. Rev. Lett.* **86** 5870

- [12] Cochrane P T, Milburn G J, and Munro W J 1999 Macroscopically distinct quantum-superposition states as a bosonic code for amplitude damping *Phys. Rev. A* **59** 2631
- [13] Munro W J, Nemoto K, Milburn G J, and Braunstein S L 2002 Weak-force detection with superposed coherent states *Phys. Rev. A* **66** 023819
- [14] Barnum H, Knill E, Ortiz G and Viola L 2002 Generalizations of entanglement based on coherent states and convex cones *Preprint quant-ph/0207149*
- [15] Thorne K S 1987 in *300 Years of Gravitation*, eds. Hawking S W and Israel W (Cambridge: Cambridge University Press)
- [16] Braginsky V B 1968 *Sov. Phys. JETP* **26** 831; Braginsky V B 1972 in *Physical Experiments with Test Bodies* NASA Technical Translation TT F-672 (Springfield: U.S. Technical Information Service).
- [17] Caves C M 1981 Quantum-mechanical noise in an interferometer *Phys. Rev. D* **23** 1693
- [18] Braginsky V B and Khalili F Ya 1992 *Quantum Measurements* (Cambridge: Cambridge University Press).
- [19] Caves C M, Thorne K S, Drever R W P, Sandberg V D and Zimmermann M 1980 On the measurement of a weak classical force coupled to a quantum-mechanical oscillator. I. Issues of principle *Rev. Mod. Phys.* **52** 341
- [20] Bocko M F and Onofrio R 1996 On the measurement of a weak classical force coupled to a harmonic oscillator: experimental progress *Rev. Mod. Phys.* **68** 755
- [21] Yuen H P 1983 Contractive states and the standard quantum limit for monitoring free-mass positions *Phys. Rev. Lett.* **51** 719
- [22] Lynch R 1984 Contractive states and the standard quantum limit for monitoring free-mass positions *Phys. Rev. Lett.* **52** 1729; 1985 Repeated contractive-state position measurements and the standard quantum limit *ibid.* **54** 1599
- [23] Caves C M 1985 Defense of the standard quantum limit for free-mass position *Phys. Rev. Lett.* **54** 2465
- [24] Ozawa M 1988 Measurement breaking the standard quantum limit for monitoring free-mass position *Phys. Rev. Lett.* **60** 385; Realization of measurement and the standard quantum limit *Squeezed and Nonclassical Light* eds. Tombesi P and Pike E R (New York: Plenum) 263-286
- [25] Ni W-T 1986 Quantum measurements and the standard quantum limit *Phys. Rev. A* **33** 2225
- [26] Bondurant R S 1986 Reduction of radiation-pressure-induced fluctuations in interferometric gravity-wave detectors *Phys. Rev. A* **34** 3927
- [27] Braginsky V B, Gorodetsky M, Khalili F Ya, Matsko A B, Thorne K S and Vyatchanin S P The noise in gravitational-wave detectors and other classical force measurements is not influenced by test mass quantization *Preprint gr-qc/0109003*
- [28] Ozawa M Universally valid reformulation of the Heisenberg uncertainty principle on noise and disturbance in measurement 2002 *Preprint quant-ph/0207121*
- [29] For a recent review of the worldwide effort to detect gravitational waves with interferometric techniques see for instance: *Proceedings of the 4th Edoardo Amaldi Conference on Gravitational Waves*, University of Western Australia, Perth, Western Australia (8-13 July 2001) ed. D. Blair, published in 2002 *Class. Q. Grav.* **19** 1227-2049
- [30] Caves C M 1986 Application of squeezed-state light to high-precision interferometry *J. Opt. Soc. Am.* **A3** P37
- [31] Ansari N A, Di Fiore L, Man'ko M A, Man'ko V I, Solimeno S and Zaccaria F 1994 Quantum limits in interferometric gravitational-wave antennas in the presence of even and odd coherent states *Phys. Rev. A* **49** 2151
- [32] Kimble H J, Levin Y, Matsko A B, Thorne K S and Vyatchanin S P V Conversion of conventional gravitational-wave interferometers into quantum nondemolition interferometers by modifying their input and/or output optics 2001 *Phys. Rev. D* **65** 022002
- [33] Storey P, Sleator T, Collett M and Walls D 1994 Contractive states of a free atom *Phys. Rev. A* **49** 2322
- [34] From a quantum-mechanical point of view, it is interesting to note that the correlation coefficient $\Delta_{xp}^2(0)$ is also directly related to the integral of $xj(x)$, $j(x)$ being the standard probability current of the initial wavefunction, see for instance Gottfried K 1996 *Quantum Mechanics* (Reading, MA: Benjamin)
- [35] Vitali D, Mancini L, Ribichini L and Tombesi P 2002 Mirror quiescence and high-sensitivity position measurements by feedback *Phys. Rev. A* **65** 063803
- [36] Zurek W H 2001 Sub-Planck structure in phase space and its relevance for quantum decoherence *Nature*

412 712

- [37] Gordon J P and Louisell W H 1966 in *Physics of Quantum Electronics* Kelly P L, Lax B and Tannenwald P E, eds. (New York: McGraw-Hill)
- [38] Kraus K 1983 *States, Effects, and Operations: Fundamental Notions of Quantum Theory* (Berlin: Springer-Verlag)
- [39] Yurke B and Stoler D 1988 The dynamic generation of Schrödinger cats and their detection *Physica B* **151** 298
- [40] Yurke B and Stoler D 1986 Generating quantum-mechanical superpositions of macroscopically distinguishable states via amplitude dispersion *Phys. Rev. Lett.* **57** 13
- [41] Schleich W, Pernigo M and Fam Le Kien 1991, Nonclassical state from two pseudoclassical states, *Phys. Rev. A* **44** 2172
- [42] Song S, Caves C M and Yurke B 1990 Generation of superpositions of classically distinguishable states from optical back-action evasion *Phys. Rev. A* **41** 5261
- [43] Monroe C, Meekhof D M, King B E and Wineland D J 1996 A “Schrödinger cat” superposition state of an atom *Science* **272** 1131
- [44] Rouse R, Han S Y and Lukens J E 1995 Observation of resonant-tunneling between macroscopically distinct quantum levels *Phys. Rev. Lett.* **75** 1614
- [45] Nakamura Y, Pashkin YA and Tsai J S 1999 Coherent control of macroscopic quantum states in a single-Cooper-pair box *Nature* **398** 786
- [46] Friedman J R, Patel V, Chen W, Tolpygo S K and Lukens J E 2000 Quantum superposition of distinct macroscopic states *Nature* **406** 43
- [47] Massini M, Fortunato M, Mancini S, Tombesi P and Vitali D 2000 Schrödinger-cat entangled state reconstruction in the Penning trap, *New Journal of Physics* **2**, 20.1
- [48] Armour A D, Blencowe M P and Schwab K C 2002 Entanglement and decoherence of a micromechanical resonator via coupling to a Cooper-pair box *Phys. Rev. Lett.* **88** 148301
- [49] Marshall W, Simon C, Penrose R and Bouwmeester D 2002 Towards quantum superposition of a mirror, *Preprint quant-ph/0210001*
- [50] Fabre C, Pinard M, Bourzeix S, Heidmann A, E. Giacobino E and Reynaud S 1994 Quantum-noise reduction using a cavity with a movable mirror *Phys. Rev. A* **49** 1337
- [51] Mancini S and Tombesi P 1994 Quantum noise reduction by radiation pressure *Phys. Rev. A* **49** 4055
- [52] Heidmann A and Reynaud S 1994 Photon noise-reduction by reflection from a movable mirror *Phys. Rev. A* **50**, 4243; Pinard M, Fabre C, Giacobino E, Heidmann A, Reynaud S 1995 Reduction of quantum-noise by a cavity with a mobile mirror *Ann. Physique* **20** 133
- [53] Mancini S, Man’ko V I and Tombesi P 1997 Ponderomotive control of quantum macroscopic coherence *Phys. Rev. A* **55** 3042
- [54] Bose S, Jacobs K and Knight P L 1997 Preparation of nonclassical states in cavities with a moving mirror, *Phys. Rev. A* **56** 4175
- [55] Zheng S B 2000 Realization of strong squeezing for a macroscopic oscillator *Commun. Theor. Phys.* **33** 510
- [56] Cirac I, Lewenstein M, Molmer K and Zoller P 1998 Quantum superposition states of Bose-Einstein condensates *Phys. Rev. A* **57** 1208
- [57] Gordon D and Savage M 1999 Creating macroscopic quantum superpositions with Bose-Einstein condensates *Phys. Rev. A* **59** 4623
- [58] Santarelli G, Laurent Ph, Lemonde P, Clairon A, Mann A G, Chang S, Luiten A N and Salomon C 1999 Quantum projection noise in an atomic fountain: a high stability Cesium frequency standard *Phys. Rev. Lett.* **82** 4619
- [59] Viola L and Onofrio R 1997 Testing the equivalence principle through freely falling quantum objects *Phys. Rev. D* **55** 455
- [60] Paz J P and Zurek W H 2000 Environment-induced decoherence and the transition from quantum to classical 72nd Les Houches Summer School on “Coherent Matter Waves”, *Preprint quant-ph/0010011*
- [61] Jung R, Ingold G-L and Grabert H 1985 Long-time tails in quantum Brownian motion *Phys. Rev. A* **32** 2510
- [62] Hakim V and Ambegaokar V 1985 Quantum theory of a free particle interacting with a linearly dissipative environment *Phys. Rev. A* **32** 423
- [63] Tessieri L and Wilkie 2002 Suppression of decoherence via strong intra-environmental coupling *Preprint*

quant-ph/0207051

- [64] Viola L and Lloyd S 1998 Dynamical suppression of decoherence in two-state quantum systems *Phys. Rev. A* **58** 2733; Viola L, Knill E and Lloyd S 1999 Dynamical decoupling of open quantum systems *Phys. Rev. Lett.* **82** 2417
- [65] Vitali D and Tombesi P 1999 Using parity kicks for decoherence control *Phys. Rev. A* **59** 4178
- [66] Dalvit D A R, Dziarmaga J, and Zurek W H 2000 Decoherence in Bose-Einstein condensates: Towards bigger and better Schrödinger cats *Phys. Rev. A* **62** 013607

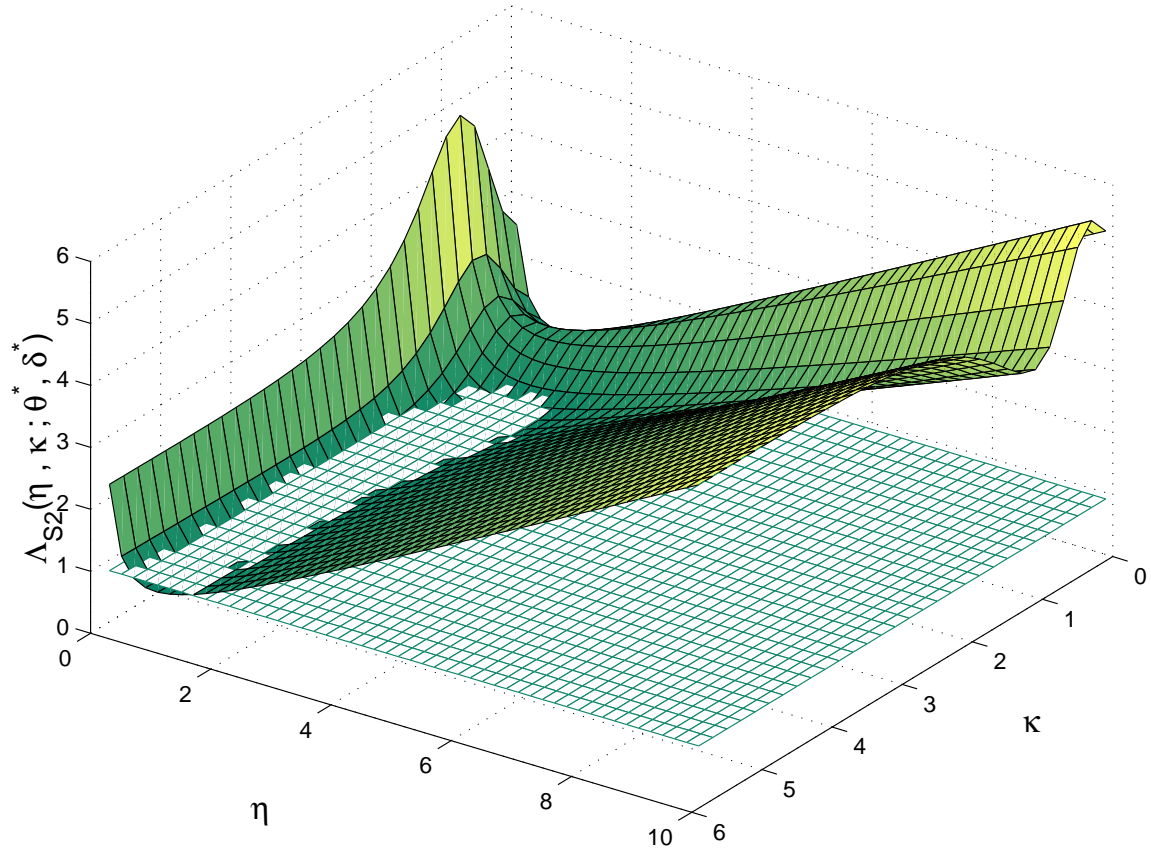


FIG. 1: The dependence of the contractivity figure of merit Λ_{S_2} upon the effective time η and κ for optimal values $\theta^* \simeq 127^\circ$ and $\delta^* \simeq 0.49$. The intersection with the plane at constant $\Lambda_{S_2} = 1$ is also evidenced, showing the existence of an island where the variance of a Schrödinger cat state maintains values smaller than the SQL.

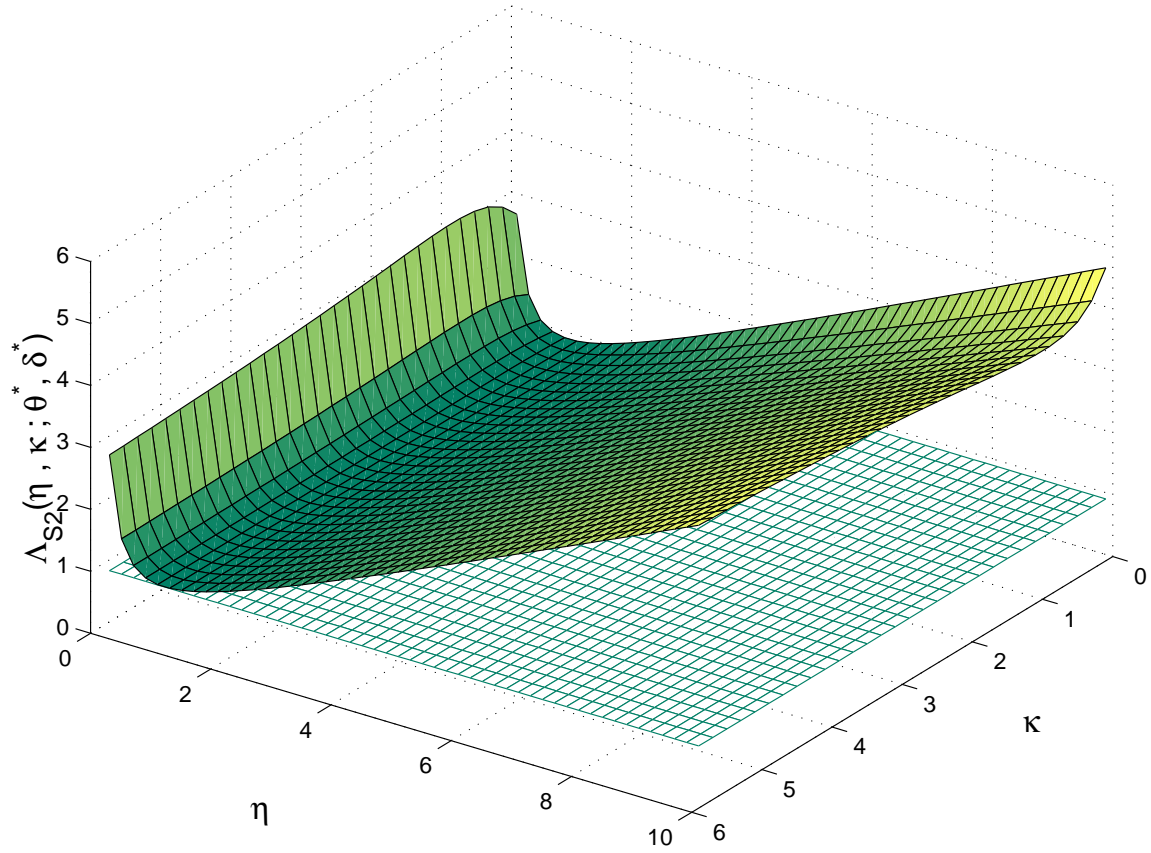


FIG. 2: The dependence of the contractivity figure of merit Λ_{S2} upon the effective time η and κ for $\theta = 0^\circ$ and $\delta^* \simeq 0.49$ as in Fig. (1). No region with $\Lambda_{S2} < 1$ is present in this case, therefore excluding any contractivity for the corresponding Schrödinger cat state.

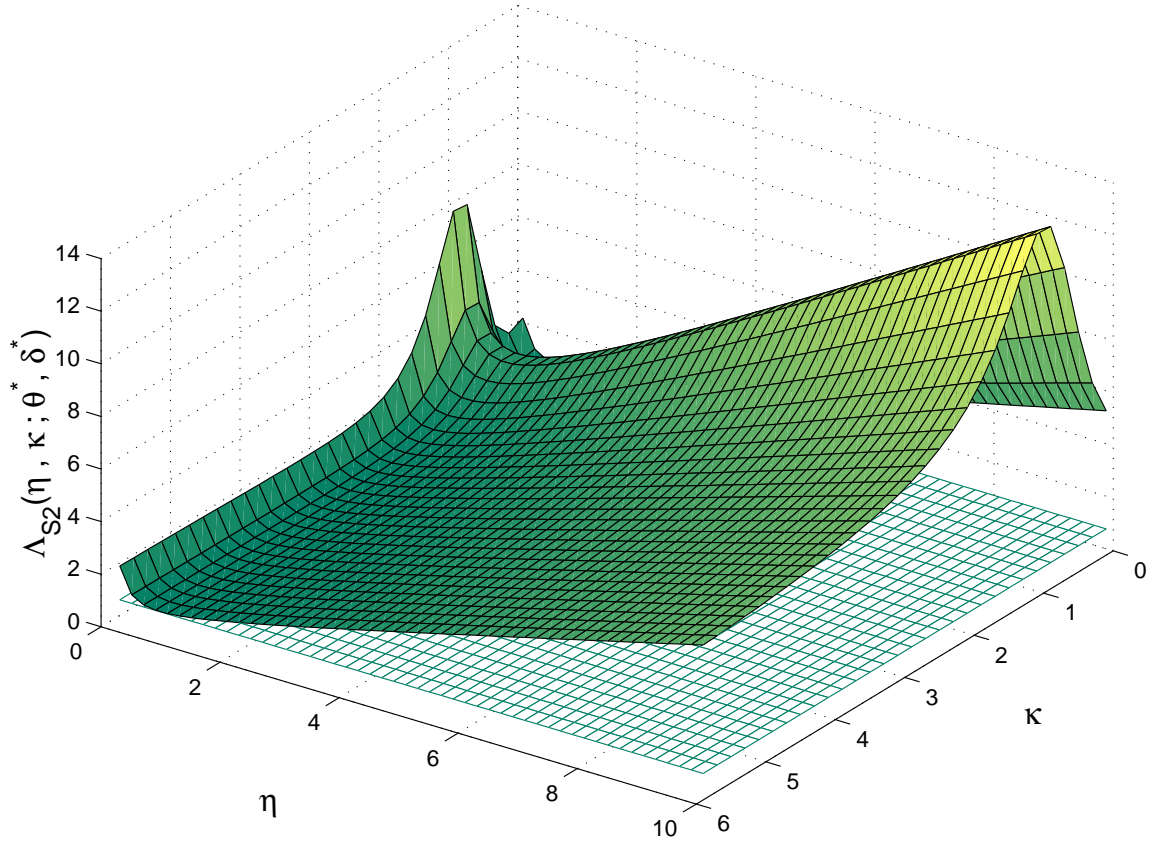


FIG. 3: As figure (2), but for $\theta = 180^\circ$.

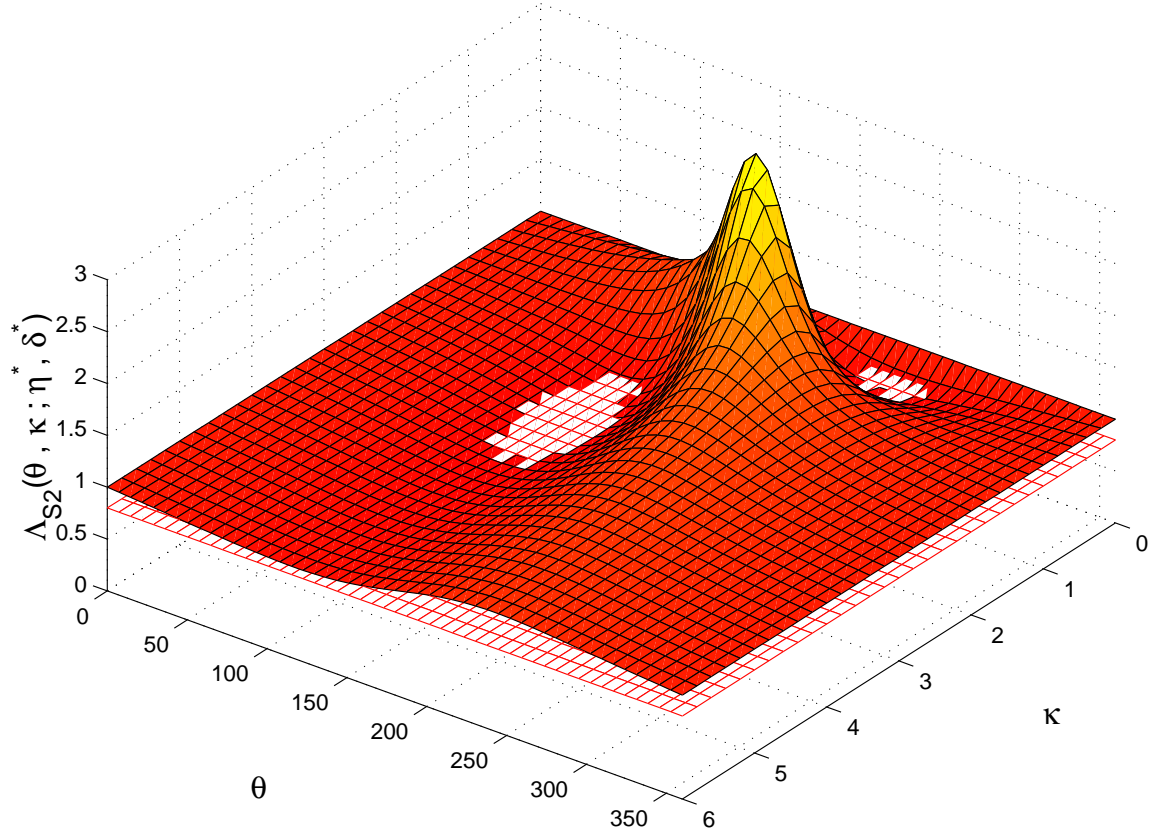


FIG. 4: The dependence of the contractivity figure of merit Λ_{S_2} upon θ and κ for optimal values $\eta^* \simeq 1.105$ and $\delta^* \simeq 0.49$. The two islands result from the section at constant $\Lambda_{S_2} = 0.8$, and are connected via the relationship given in equation (34).

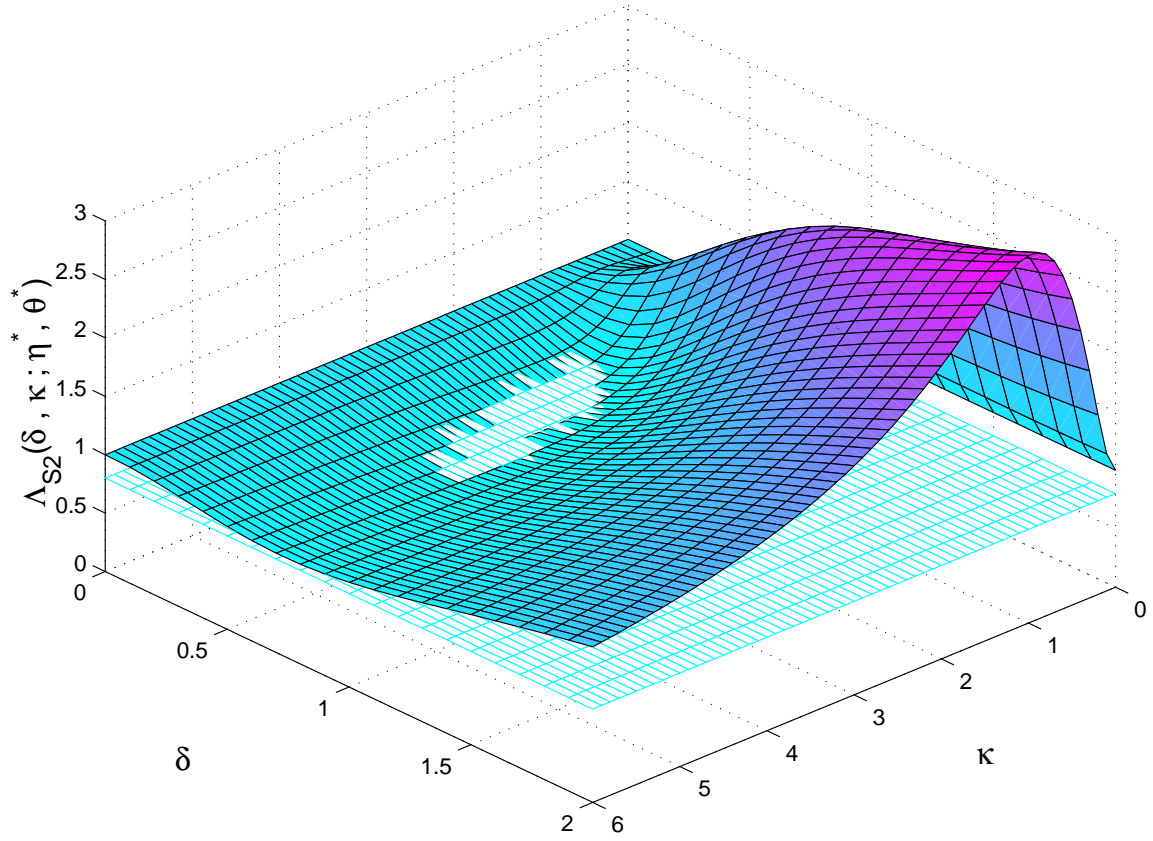


FIG. 5: The dependence of the contractivity figure of merit Λ_{S_2} upon κ and δ for optimal values $\eta^* \simeq 1.105$ and $\theta^* \simeq 127^\circ$. As in figure (4), the intersection with the plane $\Lambda_{S_2} = 0.8$ is also displayed for reference.

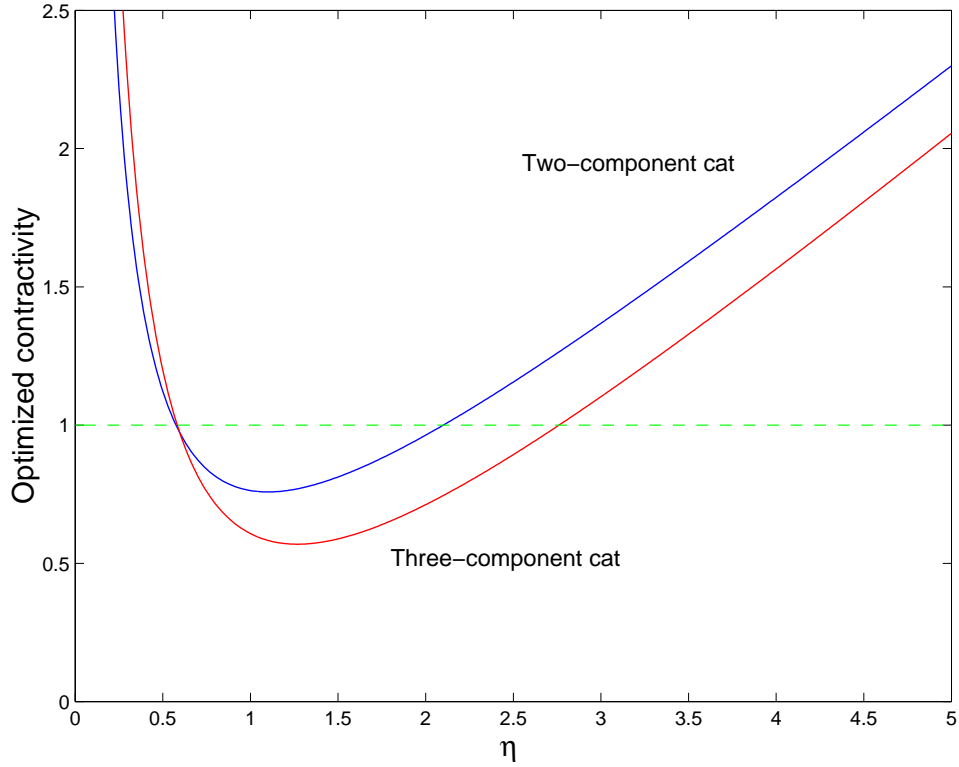


FIG. 6: Comparison of the optimized contractivity figures of merit $\Lambda_{S_2}^*$ (solid blue) and $\Lambda_{S_3}^*$ (solid red) versus rescaled time for two- and three-component cat states as in equations (19) and (36), respectively. Except for the time, all the parameters are set to their optimal values as found upon minimization of the appropriate relative variance function. Note that lower values are attained by $\Lambda_{S_3}^*$ over a wider time interval than $\Lambda_{S_2}^*$. For reference, the unity value of a non-contractive state (dashed green) is also depicted.

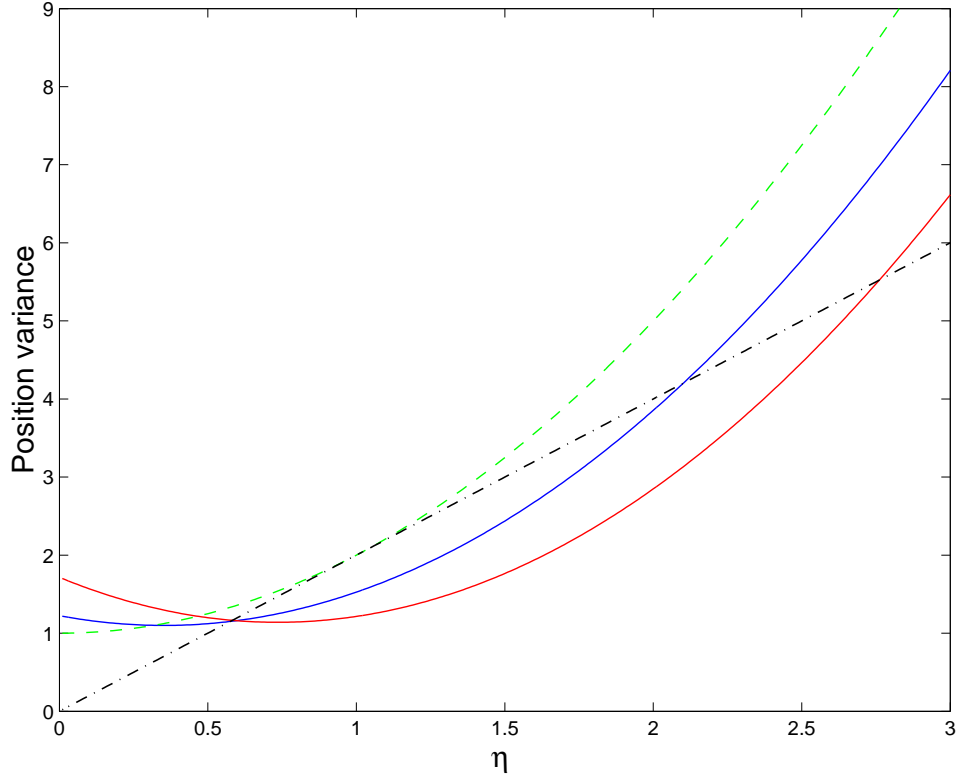


FIG. 7: The dependence of the position variance $\Delta x_{S_2}^2$ (solid blue) and $\Delta_{S_3}^2$ (solid red) versus rescaled time for two- and three-component cat states. The variance is evaluated in units of $\Delta_0^2/2$, which is the width of the probability distribution for each single Gaussian component of the cat. Except for the time, all the remaining parameters are set to the values maximizing contractivity as given in equations (35) and (47), respectively. For comparison, the variance of a single-Gaussian state evolving as in equation (48) from an initial variance $\Delta x^2(0) = \Delta_0^2/2 = 1/2$ (dashed green) is also depicted in the same units. The SQL behavior corresponds, in these units, to a line (dash-dotted black) with slope 2 which is tangent to the Gaussian curve at $\eta = 1$ and intersects the contractive curves as shown.